Chapter 15
Action Potentials: Summing Up the Effect of Loads of Ion Channels

In this final chapter we will use the theoretical drugs developed in various chapters above for whole cell simulations. So far we have studied very small parts of a cell. We started by studying the dynamics going on in a single dyad; see Fig. 2.1. The size of one dyad is less than 1/1,000 μm^3 [3] and we have been concerned with the concentration of calcium ions in this small volume. We have also studied the voltage dynamics in the vicinity of a single ion channel. The size of a single channel is about 1 nm. Now we address what is going on in a whole cell and it is important to realize that, compared to the single dyad and the single ion channel, the whole cell is huge; a normal ventricular cell is about 30,000 μm^3 [3], or on the order of 30 million times larger than the single dyad.

In the analysis of single channels, we have regarded the state of a channel as a stochastic variable. In the whole cell, however, the effect of a huge number of channels is added and the sum can be modeled using deterministic equations. We will still use the same Markov model formalism in terms of reaction schemes to formulate the models, but now we will use the associated master equations (see page 5) to define the open probability of the channel. Thus we need to solve deterministic systems of ordinary differential equations to find the open probability as a function of time.

Since the state of the channels will be represented using Markov model reaction schemes, we can study mutations in the same manner as we did for the single channel case. Therefore, we can use the results we derived above regarding optimal theoretical drugs for the single channel case for the whole cell case as well. The reasoning behind this was indicated earlier: If a mathematical model of a cell is constructed by using models of a huge number of single channels and we can repair the function of each single channel, the whole cell will be repaired.

In this chapter we will start by introducing a model of the action potential of the whole cell. We will focus on a simplified model that will merely represent the action potential in a qualitatively relevant manner; it will not represent any particular

A. Tveito, G.T. Lines, *Computing Characterizations of Drugs for Ion Channels and Receptors Using Markov Models*, Lecture Notes in Computational Science and Engineering 111, DOI 10.1007/978-3-319-30030-6_15

action potential in a quantitatively correct manner. Using numerical experiments, we will show that the model provides reasonable results for both wild type and various mutations. Finally, we will use the optimal theoretical drugs derived above and see that the effect of various mutations can be repaired using the theoretical drugs.

15.1 Whole Cell Action Potential Model

Our aim is now to introduce a reasonably simple action potential model for a whole cell. We will use the building blocks developed above and add some new features in order to get an action potential that is qualitatively reasonable.

The model consists of six main variables: v, c_e, c_c, c_d, c_j, and c_n. Here v, as usual, denotes the transmembrane potential given in mV. All the other variables are concentrations given in μM; c_e is the extracellular calcium concentration, c_c is the cytosolic concentration, c_d is the concentration of the dyad, c_j is the concentration of the JSR, and finally c_n is the concentration of the NSR; see Fig. 15.1. In addition to these six main variables, we will have variables associated with various Markov models; all these variables are between zero and one; they also denote probabilities and they have no unit. The transmembrane potential is governed by the equation

$$Cv' = -(I_{Na} + I_{Ca} + I_K + I_0) \tag{15.1}$$

where the minus sign is according to convention in the field. Here C denotes the capacitance and is simply a constant that will be specified below. The current I_0 represents a stimulus of the cell and we will use it below to initiate action potentials.

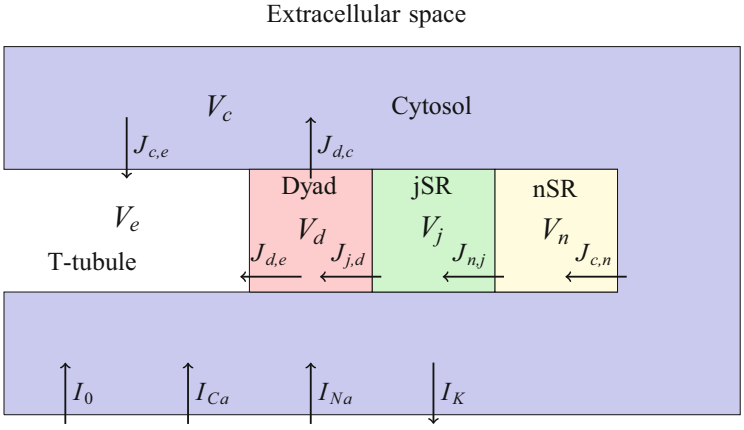

Fig. 15.1 Sketch of the calcium dynamics and the fluxes and pumps involved. The volumes of the cytosol, the dyad, the junctional sarcoplasmic reticulum (JSR) and the network sarcoplasmic reticulum (NSR) are V_c, V_d, V_j, and V_n, respectively

The sodium current I_{Na}, the calcium current I_{Ca}, and the potassium current I_K need some attention and will be handled separately.

In addition to the transmembrane potential, we need to keep track of all five calcium concentrations. By considering Fig. 15.1, we see that the cytosolic concentration can change in three ways[1]: (1) Calcium may diffuse into the cytosolic space from the dyad,[2] leading to an increase in the cytosolic concentrations; (2) it can be pumped from the cytosol into the NSR and thereby reduce the cytosolic concentration; or, finally, (3) it can be pumped out to the extracellular space, thereby reducing the cytosolic concentration. The calcium concentration of the NSR, c_n, will be increased as calcium is pumped into this space from the cytosol and reduced by diffusion into its neighboring space, the JSR. In the JSR the calcium concentration will increase through diffusion from the NSR and be reduced when calcium is released through the ryanodine receptor (RyR) into the dyadic space. Finally, the concentration in the dyad will increase when calcium is released from the JSR to the dyad; it will be reduced as calcium diffuses out to the cytosol and finally it will be increased when calcium is released into the dyad through the L-type calcium channels (LCCs). In mathematical terms, we get the following system of equations:

$$V_c c_c' = J_{d,c} - J_{c,n} - J_{c,e}, \tag{15.2}$$

$$V_n c_n' = J_{c,n} - J_{n,j}, \tag{15.3}$$

$$V_j c_j' = J_{n,j} - J_{j,d}, \tag{15.4}$$

$$V_d c_d' = J_{j,d} - J_{d,c} - J_{d,e}. \tag{15.5}$$

$$V_e c_e' = J_{c,e} + J_{d,e}. \tag{15.6}$$

Here the notation $J_{x,y}$ denotes a flux of calcium from space x to space y. So $J_{d,c}$ denotes the flux of calcium from the dyad (d) to the cytosol (c) and, similarly, $J_{d,e}$ denotes the flux of calcium from the dyad (d) to the extracellular (e) space. Here V_x denotes the volume fraction occupied by the space x (see Table 15.1). The total amount of calcium in the system is given by

$$c = V_c c_c + V_n c_n + V_j c_j + V_d c_d + V_e c_e. \tag{15.7}$$

[1]This is a major simplification; many other things can happen to calcium but this rough description is sufficient for our purposes.

[2]It is important to recall here that when we talk about the dyad now, we really refer to a space representing the sum of all the dyads of the cell. So what used to be a very tiny place is not so tiny anymore.

15.1.1 Conservation of Calcium

It follows from the system (15.2)–(15.6) that

$$c' = 0, \tag{15.8}$$

so the total amount of calcium is conserved no matter how the calcium dynamics of the cell are organized.

15.1.2 Definition of Calcium-Related Fluxes

We need to define all the fluxes entering the system (15.2)–(15.6) and we start with the simple diffusion fluxes. Some of them have been used in earlier chapters, but we need a little more notation here, so we redefine all the terms.

15.1.2.1 Flux $J_{d,c}$ from the Dyad to the Cytosol

We assume that the pure diffusion flux from the dyad to the cytosol can be written as

$$J_{d,c} = k_{d,c}\,(c_d - c_c)\,. \tag{15.9}$$

Here we assume that $k_{d,c}$ is a constant and the value used in our computations is given in Table 15.2.

15.1.2.2 Flux $J_{n,j}$ from the NSR to the JSR

Similarly, we assume that the diffusion flux from the NSR to the JSR can be written as

$$J_{n,j} = k_{n,j}\left(c_n - c_j\right), \tag{15.10}$$

where $k_{n,j}$ is assumed to be a constant (see Table 15.2).

Table 15.1 The table shows the relative size of the intracellular spaces. Note that the volume fractions of the intracellular space add up to 100 %. In addition, V_e represents 100 % of the extracellular space. We assume that both the extracellular space and the total intracellular space are 30.4 pL

V_d	0.1 %
V_j	0.3 %
V_n	1 %
V_c	98.6 %

Table 15.2 Constants used to define the fluxes between the different spaces. The constants are in units of 1/ms

$k_{c,n}$	0.01
$k_{j,d}$	0.01
$k_{d,c}$	0.001
$k_{d,e}$	0.0001
$k_{n,j}$	0.0001
$k_{c,e}$	0.00001

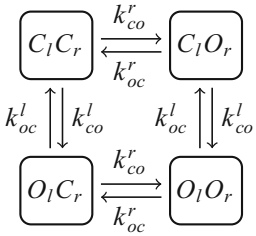

Fig. 15.2 Markov model including four possible states: C_lC_r (both closed), C_lO_r (LCC closed, RyR open), O_lO_r (both open), and O_lC_r (LCC open, RyR closed)

Table 15.3 Reaction rates used in the Markov model illustrated in Fig. 15.2. As usual, $\mu \geq 1$ denotes the mutation severity index of the RyR and $\eta \geq 1$ denotes the mutation severity index of the LCC

RyR	LCC
$k^r_{co}(c_d, c_j) = \mu \frac{c_d^4}{K(c_j)^4 + c_d^4}$ ms^{-1}	$k^l_{co}(v) = \eta\, l_\infty(v)/\tau_l$
$k^r_{oc} = 1$ ms^{-1}	$k^l_{oc}(v) = (1 - l_\infty(v))/\tau_l$
$K(c_j) = 20 + 1000(\frac{1000 - c_j}{600})^2$	$l_\infty(v) = \exp(-(\frac{v-55}{10})^2)$ $\tau_l = 1$ ms

15.1.2.3 RyR Flux $J_{j,d}$ from the JSR to the Dyad

The flux from the JSR to the dyad can be written in the form

$$J_{j,d} = o_{j,d} k_{j,d} \left(c_j - c_d\right), \tag{15.11}$$

where, as usual, $o_{j,d}$ is governed by a Markov model and $k_{j,d}$ is a constant giving the speed of diffusion when the RyR channel (situated between the JSR and the dyad) is open.

The variable $o_{j,d}$ is governed by the Markov model used in Chap. 8. For convenience the Markov model is repeated here in Fig. 15.2 and the functions used in the model are given in Table 15.3. Note that $o_{j,d}$ is the probability of being in the state C_lO_r or the state O_lO_r of the Markov model given in Fig. 15.2.

Table 15.4 Parameters in (15.12)

F	96485.3 C mol^{-1}
R	8.3145 J mol^{-1}K^{-1}
T	310 K
v_0	13.357 mV

15.1.2.4 Flux from the Extracellular Space to the Dyad: $J_{d,e}$

This flux was introduced above (see page 128) and referred to as the Goldman-Hodgkin-Katz (GHK) flux. In the present notation, we write

$$J_{d,e} = o_{d,e} k_{d,e} \frac{c_d - c_e e^{-\frac{v}{v_0}}}{1 - e^{-\frac{v}{v_0}}} \frac{v}{v_0}. \tag{15.12}$$

Here F is Faraday's constant, R is the gas constant, and T is the absolute temperature and we have defined

$$v_0 = \frac{RT}{2F}.$$

The parameters involved in defining the $J_{d,e}$ flux are given in Table 15.4. Furthermore, $o_{d,e}$ is governed by the Markov model given in Fig. 15.2. Here $o_{d,e}$ is the probability of being in the state $O_l C_r$ or the state $O_l O_r$ of the Markov model in Fig. 15.2.

15.1.3 Definition of Calcium Pumps

The terms $J_{c,e}$ and $J_{c,n}$ remain to be defined. These terms are active fluxes, or pumps, that continuously remove calcium from the cytosol and out to the extracellular domain ($J_{c,e}$) and into the NSR ($J_{c,n}$). These pumps transport calcium against a considerable concentration gradient and the operation therefore requires energy. In our model we do not track the energy consumption and we simply introduce the pumps:

$$J_{c,e} = k_{c,e}(c_c - c_e/18000) \tag{15.13}$$

and

$$J_{c,n} = k_{c,n}(c_c - c_n/10000). \tag{15.14}$$

15.1.4 Definition of the Currents

The currents I_{Na}, I_K and I_{Ca} of (15.1) remain to be defined. Each current will be written in the form

$$I_x = o_x g_x (v - v_x),$$

where o_x is the open probability of the channel given by the continuous version of a Markov model, g_x is the maximum conductance of the channel, and v_x is the resting potential.

15.1.4.1 Sodium Current I_{Na}

The sodium current has been studied above; see Chaps. 12 and 14. The model takes the form

$$I_{Na} = o_{Na} g_{Na} (v - v_{Na}), \tag{15.15}$$

where the open probability o_{Na} is the sum of the probability of being in the O or the O^* state of the Markov model of Fig. 15.3.

15.1.4.2 Potassium Current I_K

The potassium current is written in the form

$$I_K = (o_K g_K(v) + g_{K1}(v))(v - v_K), \tag{15.16}$$

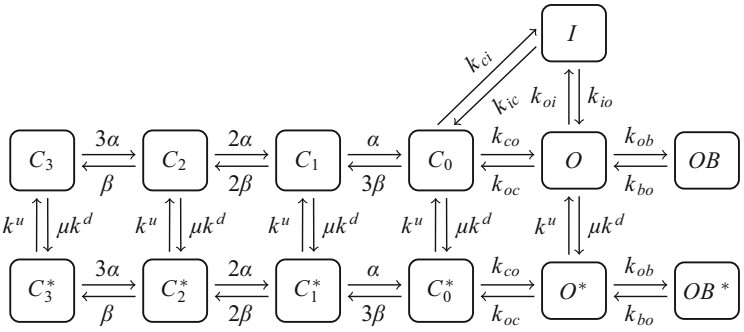

Fig. 15.3 This figure is a copy of Fig. 14.9 and it illustrates a Markov model of the mutant sodium channel. The model consists of the states O, I, OB, C_0, C_1, C_2, and C_3 of the normal mode and $OB^*, O^*, C_0^*, C_1^*, C_2^*$, and C_3^* of the burst mode (*lower part*)

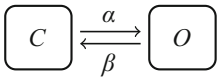

Fig. 15.4 Markov model of a potassium channel consisting of one closed and one open state

where the open probability o_K is given by the Markov model of Fig. 15.4 with rates

$$\alpha(v) = e^{-7+0.03v},$$
$$\beta(v) = e^{-8-0.03v}.$$

The voltage-dependent conductances are given by

$$g_K(v) = 0.1e^{-0.03v},$$
$$g_{K1}(v) = \frac{1}{1+e^{0.1v+10}}.$$

15.1.4.3 Calcium Current I_{Ca}

The calcium current is given by the calcium flux $J_{d,e}$ from the dyad to the extracellular space plus the flux $J_{c,e}$ from the cytosol to the extracellular space. In order to use these fluxes in the equation governing the transmembrane potential, we need convert to current density,

$$I_{Ca} = 2F\frac{V}{A}(-J_{d,e} - J_{c,e}). \tag{15.17}$$

Here $V = 30.4$ pL is the cell volume and $A = 1.4 \cdot 10^{-4}$ cm^2 is the cell area.

15.1.5 Markov Models in Terms of Systems of Differential Equations

The model of the action potential for a whole cell is a system of ordinary differential equations. For parts of the system this is clear from the equations, but for the Markov models, this may seem unclear. In Sect. 1.3 we explained how to formulate a system of ordinary differential equation associated with the reaction scheme defining a Markov model. Since the Markov models considered in the present chapter are considerably more complex, we will give one more example of this transition in order to clarify matters. To this end, consider the Markov model presented in Fig. 15.5. The associated system of ordinary differential equations governing the

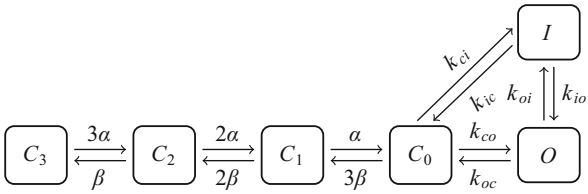

Fig. 15.5 Markov model of a wild type sodium channel consisting of an open state (O), an inactivated state (I), and four closed states ($C_0, C_1, C_2,$ and C_3)

probabilities is given by

$$
\begin{aligned}
o' &= k_{io} i + k_{co} c_0 - (k_{oc} + k_{oi})\, o, \\
i' &= k_{oi} o + k_{ci} c_0 - (k_{io} + k_{ic})\, i, \\
c_0' &= k_{oc} o + k_{ic} i + \alpha c_1 - (k_{co} + k_{ci} + 3\beta)\, c_0, \\
c_1' &= 3\beta c_0 + 2\alpha c_2 - (2\beta + \alpha)\, c_1, \\
c_2' &= 2\beta c_1 + 3\alpha c_3 - (2\alpha + \beta)\, c_2, \\
c_3' &= \beta c_2 - 3\alpha c_3.
\end{aligned}
$$

Here, o denotes the open probability of the sodium channel, c_0 is the probability of the C_0 state, and so forth. Ideally, we would write o_{Na} for o, $c_{0,Na}$ for c_0, and so forth, but it becomes clumsy. Since these variables represent probabilities, they sum to one (for all time) and we can therefore reduce the number of unknowns in the system by one.

Based on this example, it should be straightforward to formulate the system of ordinary differential equations associated with the more complex Markov model given in Fig. 15.3.

15.2 Numerical Simulations Using the Action Potential Model for Wild Type Markov Models

The complete version of the model presented above can be written in the compact form

$$
C v' = -\left(I_{Na} + I_{Ca} + I_K + I_0\right), \tag{15.18}
$$

$$
u' = F(v, u), \tag{15.19}
$$

where v is the transmembrane potential and all other variables are gathered in the vector u. The initial conditions used in the simulations are given in Table 15.5. In addition, we need to specify the applied current I_0. This current will be zero most of the time, but it will be turned on every 500 ms in order to mimic periodic stimulation

Table 15.5 Initial conditions. The Markov models for the LCC and RyR were initially set to closed and the Markov model for sodium channel was set to be in the state C_3. Starting with these conditions, the code is run for 1,000 cycles in order to generate the initial conditions used in generating the figures below. The exact numbers obtained depend upon the chosen cycle length

v	-85 mV
c_d	0.1 μM
c_c	0.1 μM
c_j	1,000 μM
c_n	1,000 μM
c_e	1,800 μM

of the cell. More specifically, we hold $I_0 = -6$ mV/ms for 5 ms at the start of each cycle.

15.2.1 Single Action Potential

In Fig. 15.6 we show the transmembrane potential and all the calcium concentration for a single action potential. There are a number of interesting effects acting together to generate the action potential. Let us consider some of them in some detail.

In Fig. 15.7 we show the first 20 ms of the computation. In the left panel we show the transmembrane potential v (upper left panel), the open probability o_{Na} (middle left panel), and the sodium current I_{Na} (lower left panel). Observe that when the cell is stimulated by the applied current I_0, the transmembrane potential increases. This increase leads to an increased open probability of the sodium channel. When the sodium channel opens, the sodium current becomes large (or very negative, to be precise), which leads to a fast increase of the transmembrane potential. As the transmembrane potential reaches its peak value (at about 15 ms), the open probability starts to decline, since the channel inactivates. In the three right panels, we show the calcium concentration of the dyad c_d (upper right panel), the calcium flux $J_{d,e}$ (middle right panel), and the open probability of the RyR channel (lower right panel). We see that when the transmembrane potential starts increasing, the calcium flux $J_{d,e}$ increases and the calcium concentration of the dyad increases. This increase leads to the increased open probability (lower right panel) of the RyR channel and therefore the dyad concentration increases rapidly.

In Fig. 15.8, we show the return to the stable equilibrium solution. In the left panel, we show the transmembrane (upper left panel), the open probability of the LCC (middle left panel), and the open probability of the gated potassium channel. After the sodium channel has switched off (see Fig. 15.7), the calcium current contributes to a continued depolarized state. However, after about 20 ms the transmembrane potential starts declining because of a substantial (positive) potassium current.

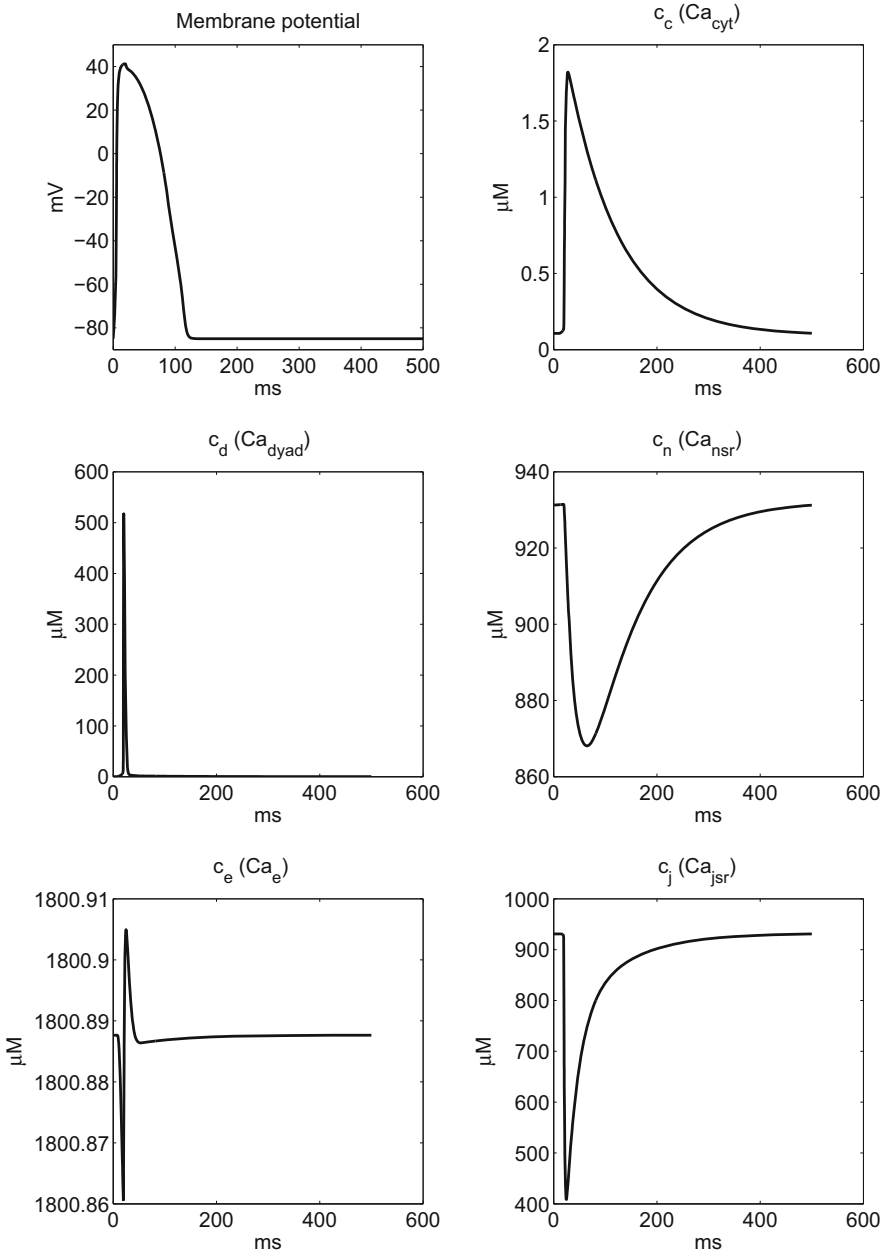

Fig. 15.6 The action potential of the model described in the present chapter. The membrane potential (*upper left*) and the dynamics of the five calcium concentrations are shown for 500 ms. The action potential is initiated by holding $I_0 = -6$ mV/ms for 5 ms. All variables return to their resting values after about 500 ms

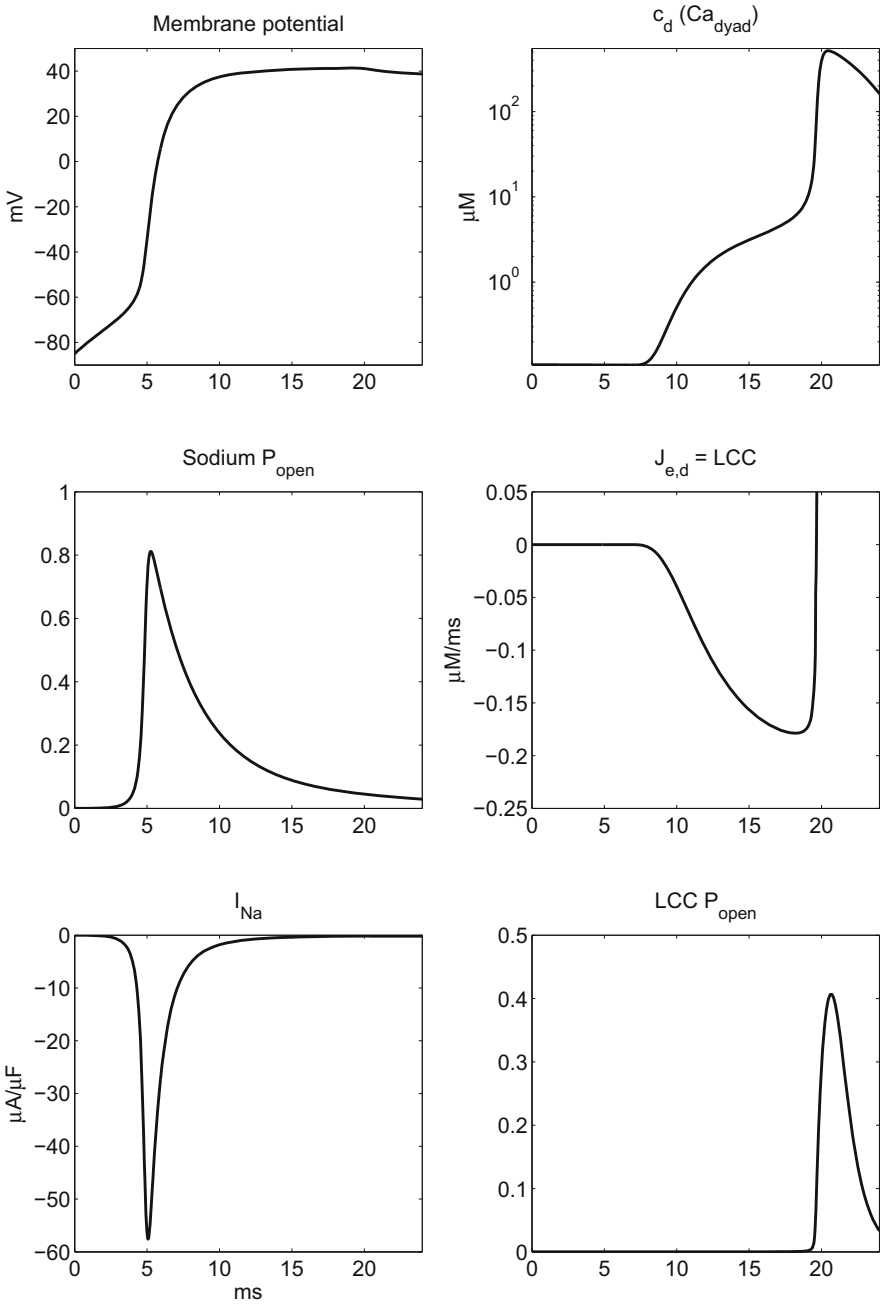

Fig. 15.7 The first 20 ms of the simulation shown in Fig. 15.6. Note the log scale in the *upper right panel*. There we see a slow rise due to the LCC opening, followed by a fast rise due to the RyR opening

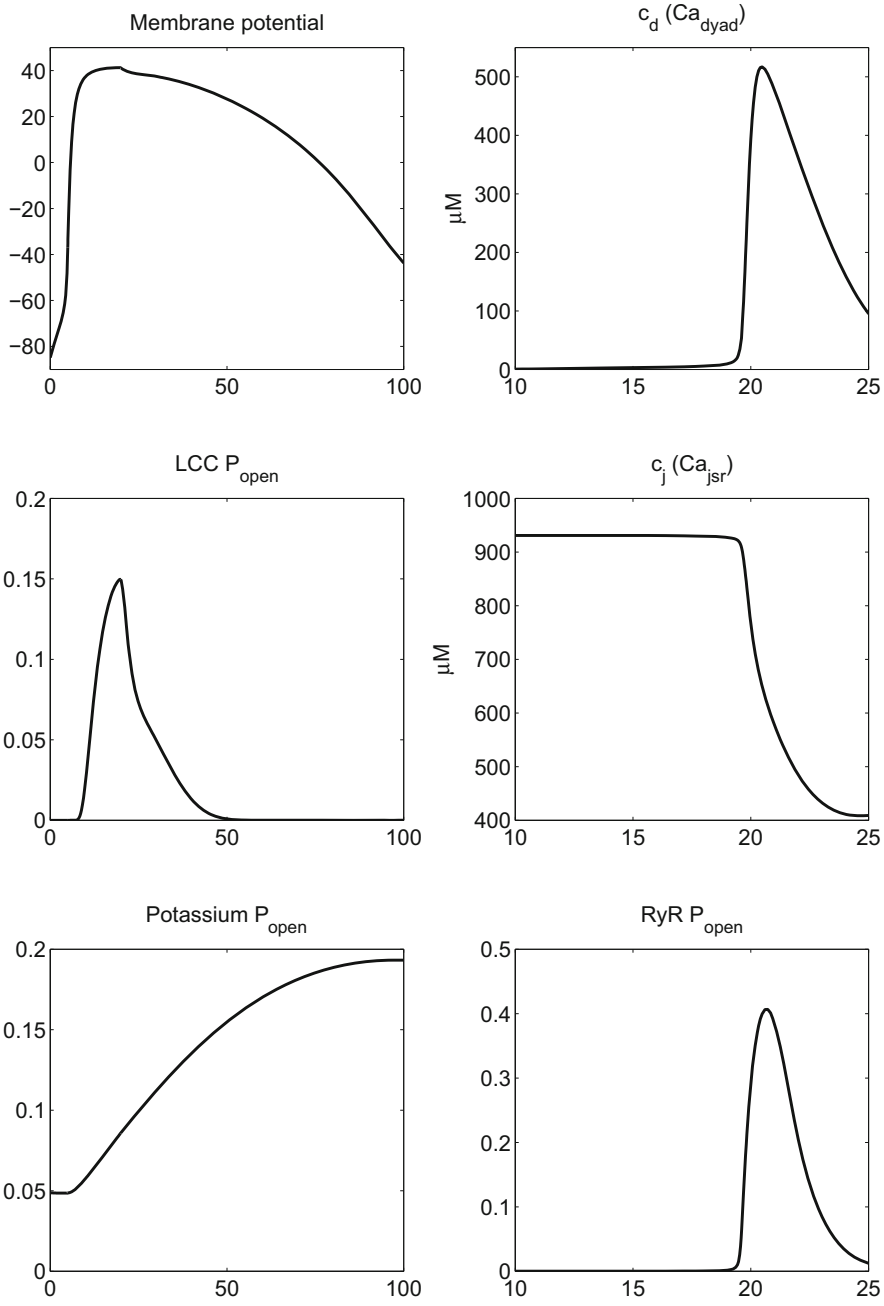

Fig. 15.8 After about 15 ms, the transmembrane potential (*upper left*) reaches its peak value and enters the plateau phase before it starts to decline toward the stable equilibrium solution

In the right panels, we follow the development of the calcium concentration of the dyad c_d (upper right panel), the calcium concentration c_j of the JSR, (middle right panel), and the open probability of the RyR channel, denoted $o_{j,d}$ (lower right panel).

15.2.2 Many Action Potentials

In Fig. 15.9, we show the action potential for a simulation running for 25,000 ms. The left panel shows the transmembrane potential v (upper left panel), the calcium concentration c_d of the dyad (middle left panel), and the extracellular calcium concentration c_e (lower left panel). From top to bottom in the right panels, we show the cytosolic calcium concentration c_c, the NSR calcium concentration c_n, and finally the JSR calcium concentration c_j. All variables return to their initial values and the rhythm seems to be perfect.

15.3 Changing the Mean Open Time of the Sodium Channel While Keeping the Equilibrium Probability Fixed Changes the Action Potential

We consider a case where we multiply all rates of the Markov model (see Fig. 15.3) of the sodium channel by the same factor. Here we use the wild type case ($\mu = 1$) and the drug parameters (k_{ob}, k_{bo}) are set to zero. This will change the mean open time, but not the equilibrium probabilities. The results are given in Fig. 15.10, where the blue line illustrates the results using default parameters, the red line represents the solution when all the rates are multiplied by 1.3, and finally the green line represents the solution when all the rates are multiplied by 0.7. We observe that the action potential changes substantially when the rates are changed (and the mean open time is changed), even though the equilibrium probabilities are kept unchanged.

15.4 Numerical Simulations Using the Action Potential Model When the Cell Is Affected by a Mutation

We will use the model of the action potential for the whole cell introduced above to study the effect of mutations. We have studied many different theoretical models of mutations earlier, but here we will limit ourselves to study the effect of one theoretical model of a sodium channel mutation, one model of a RyR mutation, and

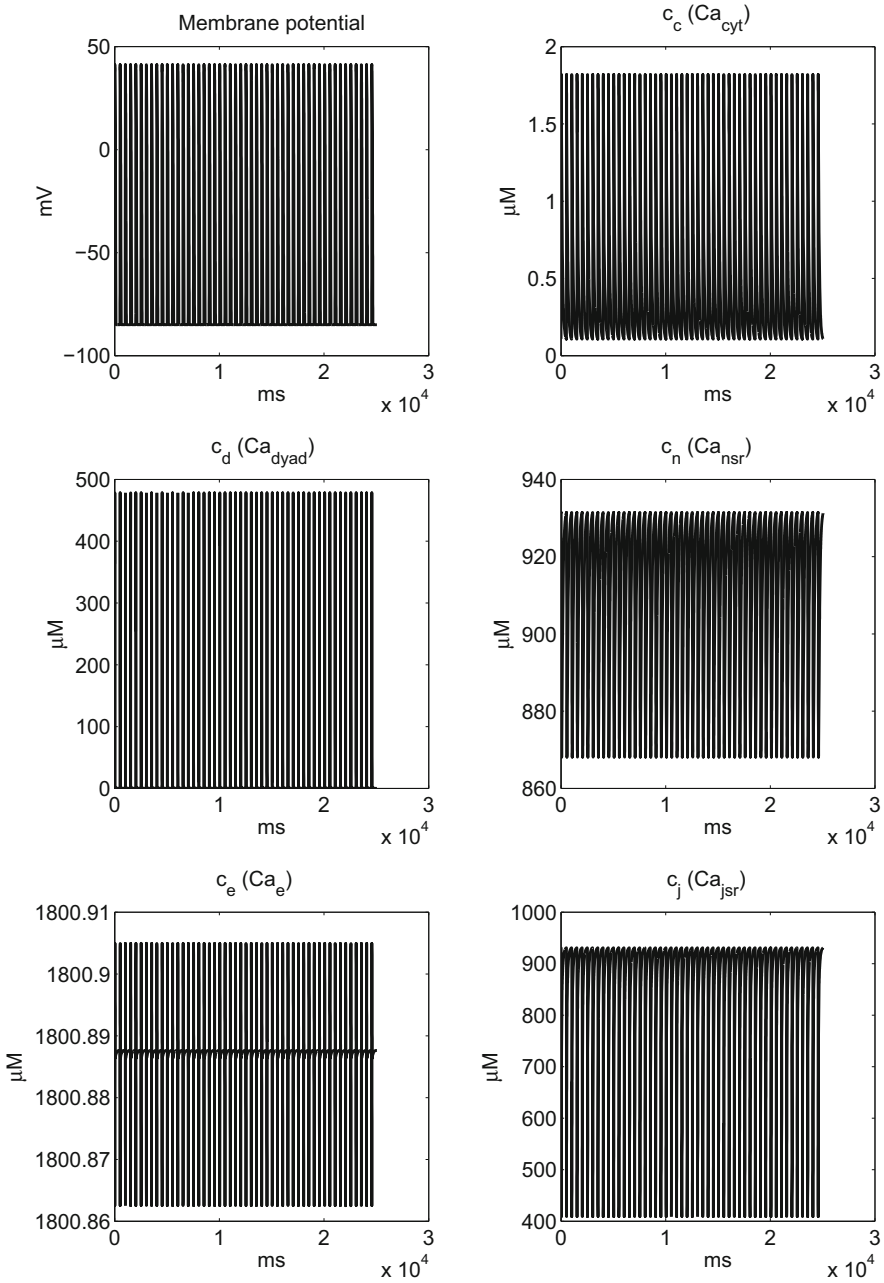

Fig. 15.9 The action potential running for 25,000 ms (50 beats). All variables return to their equilibrium values before a new action potential is initiated (every 500 ms)

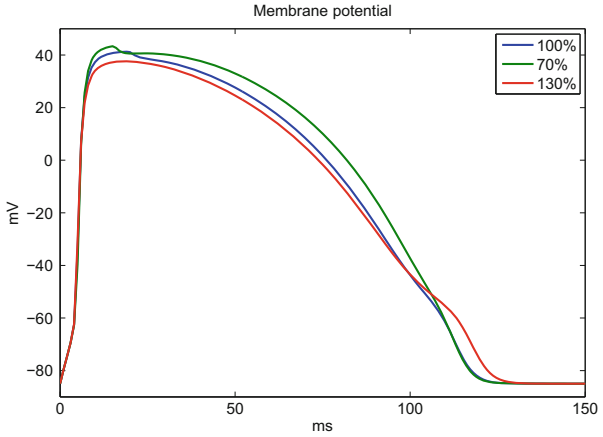

Fig. 15.10 Slower dynamics (*green*) lead to later inactivation, yielding a higher plateau. Quicker dynamics (*red*) lead to faster recovery from inactivation, allowing a stronger late current

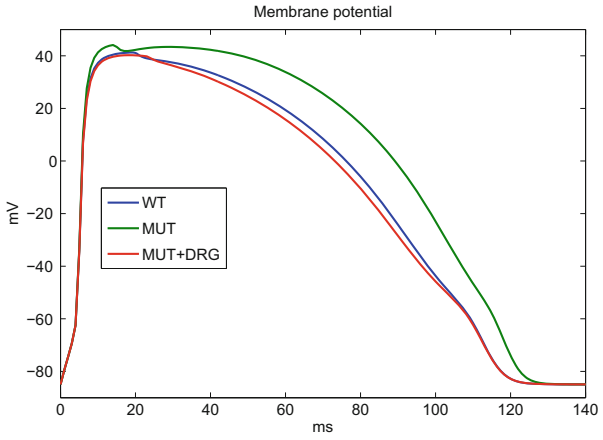

Fig. 15.11 The figure shows the action potential of the wild type (*blue*), the mutant (*green*), and the mutant after the application of the drug (*red*)

one model of an LCC mutation. We will also see how the theoretical drugs derived above handle these mutations.

15.4.1 Mutation of the Sodium Channel

We consider a mutation of the sodium channel of the form presented in Fig. 15.3. In Fig. 15.11 we show simulation results comparing the wild type ($\mu = 1$, blue), the mutant ($\mu = 10$, green), and a simulation (red) where a drug is applied to the

mutant case. The Markov model describing the open state drug is given in Fig. 15.3, where we have used drug parameters given by

$$k_{bo} = k_{io}, \text{ and } k_{ob} = (\mu - 1)\,\frac{k^d k^u k_{oi}}{(k^u + \mu k^d)\,(k^u + k^d)};$$

see (14.20) and (14.23). As in the single channel case, we observe that the theoretical drug is able to repair the effect of the mutation.

15.4.2 Mutation of the RyR

In Fig. 15.12 we have simulated mutation in the RyR using the Markov model given in Fig. 15.2. The figure shows the wild type (blue, $\mu = 1$), the mutant (green, $\mu = 3$), and the mutant where the drug has been applied (red). We have used a closed state drug computed as described in (3.5) and (3.9) and we observe that the theoretical drug is able to repair the effect of the mutation.

15.4.3 Mutation of the LCC

In Fig. 15.13 we have simulated mutation in the LCC channel, using $\eta = 3$. We model the mutation and the drug as defined in (3.5) and (3.9). As usual, k_{bc} is a free

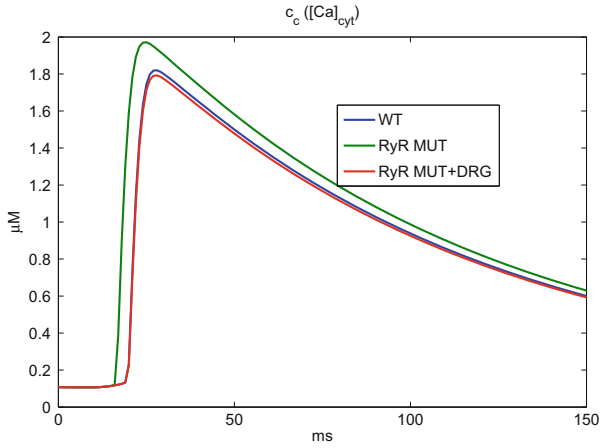

Fig. 15.12 The cytosolic calcium concentration for wild type (*blue*, $\mu = 1$), the mutant (*green*, $\mu = 3$), and the mutant after the application of the drug (*red*). We have used a closed state drug as defined in (3.5) with $k_{bc} = 0.5\ \text{ms}^{-1}$ and $k_{cb} = (\mu - 1)k_{bc}$; see (3.9)

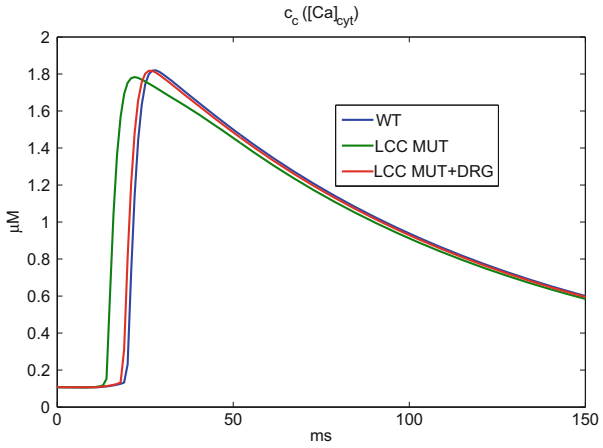

Fig. 15.13 LCC mutation. The cytosolic calcium concentration for the wild type (*blue*, $\eta = 1$), the mutant (*green*, $\eta = 3$), and the mutant case where the theoretical drug is applied (*red*). In the computations we have used $k_{bc} = 0.05\ \text{ms}^{-1}$; for larger values of k_{bc} the results overlap with the wild type case

parameter that must be chosen sufficiently large. Again, we note that the theoretical drug repairs the effect of the mutation.

15.5 Notes

1. The action potential model discussed in Sect. 15.1 and used throughout this chapter is only of qualitative relevance; no effort is made to mimic the properties of one particular cell. The field of models for the action potential is huge and growing. A great collection of models is provided by the Auckland Bioengineering Institute at the University of Auckland and their collaborators; see CellML.org. Recent models tend to be increasingly complex and hard to deal with from a mathematical perspective, but clearly the models become more and more realistic in terms of mimicking the properties of the actual action potential. As mentioned earlier, there are comprehensive introductions to the cardiac action potential, such as Rudy [74] and Rudy and Silva [75].
2. In these notes we have used Matlab as the computational platform for all our simulations. For solving ordinary differential equations we have used the ODE15s function. However, solving the ordinary differential equations modeling the single cell action potential has received a great deal of attention and numerical methods suited for this problem have been developed. An early alternative was developed by Rush and Larsen [76]; the method was improved to second by Sundnes et al. [92] and comparisons of several methods were provided by Marsh et al. [56] and Campos et al. [8]; see also Stary and Biktashev [88]. From

a programming perspective, the explicit Euler scheme is always an attractive alternative, but for stiff problems the stability requirement often excludes that method. For instance, if we use the explicit Euler method with a fixed time step to compute the solutions shown in Fig. 15.6, we need about 26,000 time-steps, whereas the ODE15s method needs 335 time steps.